

Depth-dependent evaluation of residual material properties of fire-damaged concrete

Gyu-Jin Kim and Hyo-Gyoung Kwak*

Department of Civil and Environmental Engineering, Korean Advanced Institute of Science and Technology,
291 Daehak-ro, Yuseong-gu, Daejeon 34141, Republic of Korea

(Received November 16, 2016, Revised June 21, 2017, Accepted July 28, 2017)

Abstract. In this study, fire-damaged concrete was investigated by a nonlinear resonance vibration (NRV) technique, in order to evaluate its residual material properties. For the experiments, five cubic concrete specimens were prepared and four of them were damaged at different temperatures using a furnace. With a thermal insulator wrapped at the sides of specimen, thermal gradation was applied to the samples. According to the peak temperatures and depths of the samples, nonlinearity parameters were calculated with the NRV technique before the tendency of the parameters was evaluated. In addition, compressive strength and dynamic elastic modulus were measured for each sample and a comparison with the nonlinearity parameter was carried out. Through the experimental results, the possibility of the NRV technique as a method for evaluating residual material properties was evaluated.

Keywords: fire-damaged concrete; nonlinear resonance vibration (NRV); thermal gradation; residual material property; compressive strength; dynamic elastic modulus

1. Introduction

Concrete is a widely used material because of its high compressive strength and excellent thermal resistance. However, if the concrete is exposed to high temperature for a long time, the material suffers severe damage such as internal and external cracks, delamination, and spalling (Bazant and Kaplan 1996, Choi *et al.* 2017, Zhang *et al.* 2017). As a result of this damage, the physical properties of the material also deteriorate, specifically compressive, tensile strength and elastic modulus (Yu and Lu 2015). This damage is due to the microphysical and microchemical effects of the internal cement and aggregate matrix due to the continuous high temperature exposure. According to previous research, concrete exposed to high temperature above 100°C starts to release moisture, and dehydration in cement gel occurs above 180°C. At temperatures above 500°C, decay of Ca (OH)₂ and transformation of alpha-quartz to beta-quartz proceed, as well as the collapse of ettringite structures (Alonso and Fernandez 2004, Handoo *et al.* 2002). In order to overcome these drawbacks, various experimental studies on deterioration damage of fire-damaged concrete have been carried out, and related codes have been newly improved due to improvement of the mix proportion and the incorporation of new materials (ACI 1989, ACI 1997, Tang 2017).

A variety of studies have been conducted to measure the durability and strength of fire-damaged concrete. According to the ACI report, various nondestructive testing methods

have been suggested as visual inspection and stress-wave techniques. In 2008, Kim and Kwak evaluated the elastic properties of concrete by using a surface wave (ACI 1998, Kim and Kwak 2008). Recently, nondestructive testing methods based on elastic waves have been widely applied for evaluating damaged concrete. Among these, ultrasonic pulse velocity and dynamic elastic modulus techniques use linear elastic waves to estimate the residual properties of structures. Cloni (2007) investigated a fire-damaged column with ultrasonic velocity, and Yang (2009) conducted a study on the residual compressive strength of fire-damaged concrete (Cloni *et al.* 2007, Yang *et al.* 2009). However, it has been reported that this method suffers from limited sensitivity when measuring microstructural change under a micrometer scale (Jhang 2009, Van Den Abeele *et al.* 2000a). Examples of techniques based on nonlinear ultrasonic waves, meanwhile, include higher harmonics, nonlinear resonant ultrasonic spectroscopy, and nonlinear resonance vibration. These techniques reflect the changes of the microstructure such as voids, phases, etc., and show more accurate measurement results (Park *et al.* 2017, Gomez *et al.* 2017). In previous studies, cement-based materials exposed to high temperatures were investigated with nonlinear techniques, (Payan *et al.* 2007).

In the present study, the properties of concrete exposed to high temperature were measured by temperature and depth by adopting a nonlinear resonance vibration technique. For this purpose, five concrete specimens of 300 mm×300 mm in section and 200 mm in depth were prepared, and four specimens were damaged by 200°C, 400°C, 600°C, and 800°C, respectively. The values of the nonlinearity parameter were calculated by measuring the resonant frequency of each specimen, and the changes of these values were compared and analyzed. The compressive

*Corresponding author, Professor
E-mail: khg@kaist.ac.kr

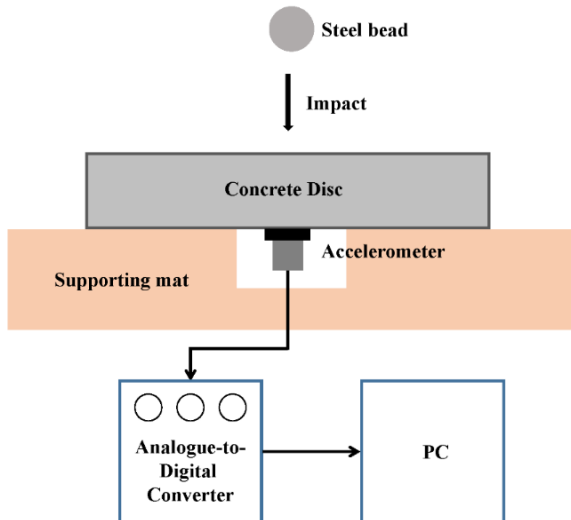


Fig. 1 Schematic illustration of NRV technique

strength was then estimated by measuring the splitting tensile strength of each specimen, with a comparison of the nonlinearity parameters and the compressive strength. In addition, the dynamic elastic modulus was estimated from the resonance frequency measurement, and the change of the dynamic modulus and the value of the nonlinearity parameter were compared. Finally, the possibility of estimating the depth-dependent material properties of fire-damaged concrete through a nonlinear resonance vibration technique was confirmed.

2. Experimental details

2.1 Nonlinear resonance vibration

In this experiment, a nonlinear resonance vibration technique was introduced to measure the changing resonance characteristics of a concrete specimen when a gradually increasing impact was applied. This technique can sufficiently reflect the nonlinear behavior of concrete and is therefore suitable for measuring the degree of damage to a specimen subjected to fire damage. In the case of a heterogeneous medium such as concrete, the relationship of stress strain exhibiting nonlinear hysteretic behavior can be expressed as the following equation.

$$E(\varepsilon(t), \dot{\varepsilon}(t)) = E_0[1 - \beta\varepsilon(t) - \alpha\{\Delta\varepsilon + \varepsilon(t) \cdot \text{sign}(\dot{\varepsilon}(t))\} + \dots] \quad (1)$$

where E is the elastic modulus, E_0 is the linear elastic modulus, ε the strain, and $\dot{\varepsilon}$ the strain rate. Also, β is the second order nonlinearity parameter of the material and α is the nonlinearity parameter according to the hysteresis and discrete memory of the material. According to the model, phenomena such as higher harmonic generation and a shift of resonant frequency occur in damaged concrete, and this can be used as a damage indicator to detect contact-type defects in a specimen (Van Den Abeele *et al.* 2000b). In this experiment, the resonant frequency was measured to calculate the value of the nonlinearity parameter (Guyer and Johnson 1999). As the amplitude of the incident impact

Table 1 Mixing proportion and compressive strength of concrete specimen

W/C (%)	Unit Weight (kg/m ³)					Strength (MPa)
	W	C	S	G	AD	
0.42	180	360	837	970	2.81	30.0



(a) Concrete specimens casted in a mold (b) Coring of damaged specimen

Fig. 2 Example of experimental process



Fig. 3 Concrete specimen fire-damaged at 200°C

increases, the resonance frequency decreases in the lower direction, and the value of the nonlinearity parameter can be calculated as follows

$$\frac{f_0 - f}{f_0} = \alpha_h \Delta\varepsilon \quad (2)$$

where $\Delta\varepsilon$ is the difference in strain between measurements, which does not change during measurement, f_0 is the resonant frequency measured when the lowest input impact

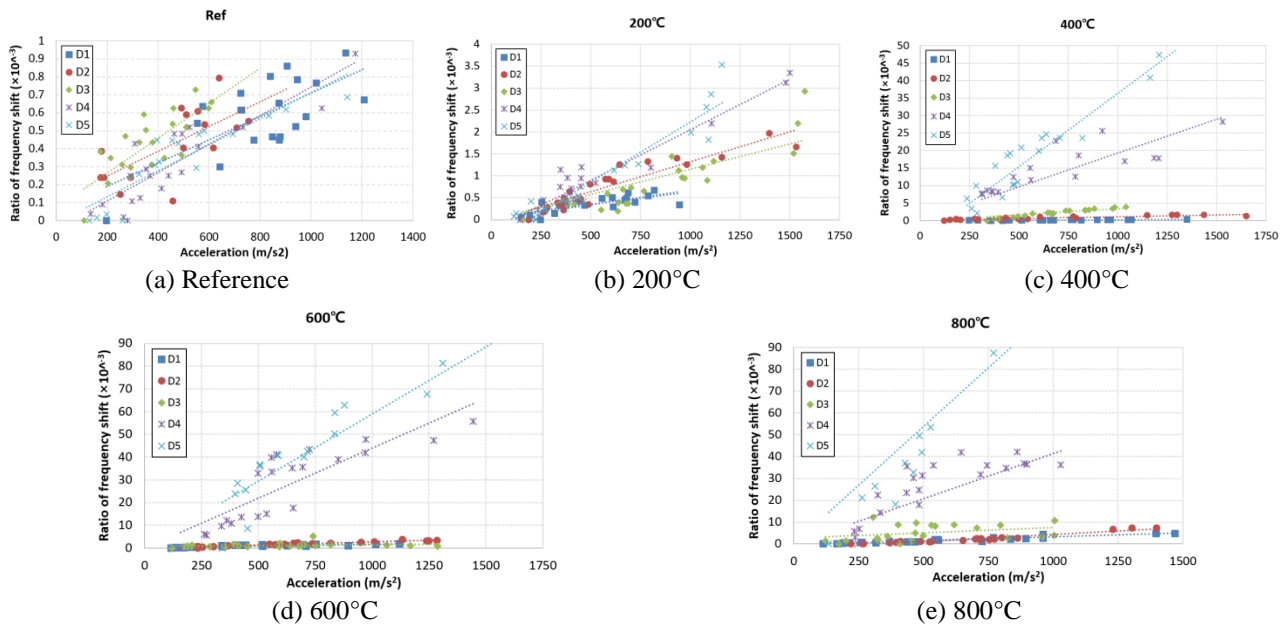


Fig. 4 Ratio of resonant frequency shift

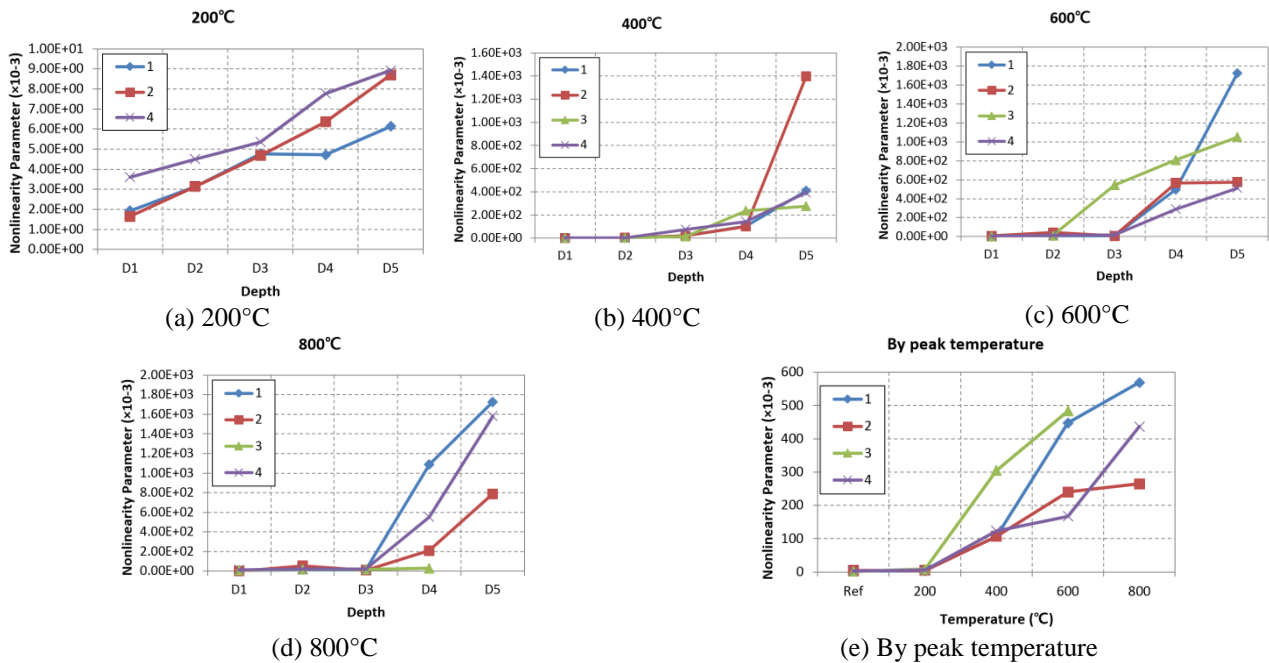


Fig. 5 Nonlinearity parameters measured by NRV

is applied, in other words, the linear resonant frequency, and f is the value of the resonance frequency measured according to the specific impact level (Van Den Abeele *et al.* 2001). Therefore, the value of the nonlinearity parameter a can be calculated through the difference between the resonant frequency values, and it is possible to evaluate the nonlinearity parameter and the degree of damage regardless of the varying linear resonant frequency of each specimen.

Fig. 1 shows a schematic illustration nonlinear resonance vibration technique. The specimen is placed horizontally on a preformed soft mat, which blocks the external noise. A steel bead with a 14 mm diameter and a

12.8 g mass is dropped onto the center of the specimen to cause fundamental resonance vibration. At this time, an appropriate height from which the steel bead is dropped should be decided due to the superimposed signals that occur with an excessively low case and additional damage problem with an overly high case. The vibration response of the specimen is measured with a shear piezo-electric accelerometer (PCB 353B15, PCB Piezotronics Inc.) attached on the opposite side with a couplant, and the peak point of each signal is recorded to obtain the resonant frequency. The signal is automatically converted and recorded by an analogue-to-digital converter (NI PXI 4472-

B, National Instruments Corp.), and saved in a PC. The time domain data are converted to a frequency domain by a fast-Fourier transformation. In order to calculate the nonlinearity parameter, the measurement is conducted 20 times with different input impacts.

2.2 Specimen preparation: Thermal gradation

Five unfilled concrete specimens are shown in Fig. 2(a), and the size of the cross section is 300 mm by 300 mm and the depth is 200 mm. In this case, the size of the cross section was made to be the same size as the section of the furnace in order to damage the test piece by depth. The concrete mixing ratio is shown in Table 1, where W/C denotes the water cement ratio, W water, C cement, S fine aggregate, G coarse aggregate, and AD admixture. The maximum aggregate size was 4 mm and the coarse aggregate was less than 25 mm. The water to cement ratio was 0.42 and the admixture was 2.81 kg/m³. The concrete specimens were cured in water for 28 days after demolding, and dried at 80°C for 24 hours to prevent spalling. The compressive strength by the test of ASTM C 39 was measured as 30 MPa (ASTM C 39-01 2001).

Fig. 3 shows the concrete specimen damaged by using a furnace at 400°C. One of the five specimens was not damaged as a reference, and the remaining four specimens were heated for 7 hours at set temperatures of 200°C, 400°C, 600°C, and 800°C, respectively. The measured time to reach the set temperature was 1 hour for 200°C, 1.5 hours for 400°C, 2 hours for 600°C, and 2.5 hours for 800°C, respectively. In the fire-damaging process, the inner side of the furnace was wrapped with a thermal insulator for thermal gradation of the test specimens. The damaged concrete was cooled for 24 hours at room temperature and coring was performed in a cylindrical shape with a 100 mm diameter and a 200 mm height, as shown in Fig. 2(b). Considering the thermal conductivity and thickness of the concrete specimens, cylindrical specimens were cut at 25 mm intervals into disc-shaped samples, where the disc nearest from the heating point was classified as D5 (the most damaged sample) and the farthest disc as D1.

3. Experimental results

3.1 Comparison of nonlinearity parameters dependent on depth and temperature

Using the nonlinear resonance vibration technique, the resonance frequency shift ratio of the specimen according to the peak temperature is illustrated in Fig. 4. The graphs from (a) to (e) indicate the measurement results at reference (no damage), 200°C, 400°C, 600°C, and 800°C, respectively, and the results in the graph are separately denoted by the depths. First, the difference of the resonance frequency is not significant with an increase of acceleration, as well as with respect to the depth of the reference specimens (Fig. 4(a)). Based on the reference, the results of the specimens damaged at different peak temperatures can be compared. Notably, the measurement results of the specimens damaged at 200°C show an observable

difference (Fig. 4(b)). Although the difference is not large compared to the reference, the result measured at D1, which is farthest from the heating point, indicates a certain level of resonance frequency decrease with increasing acceleration, and this is presumed to be caused by contact-type defects with fire damage (Park *et al.* 2015). Furthermore, the comparison results also differ according to the depths from D1 to D5, and it can be observed that the shifts gradually increase as the heating point is approached. Through the comparison, it can be seen that the concrete is finely damaged even at a relatively low temperature of 200°C, and the damage of concrete is estimated to be classified by the thermal gradation inside the specimen. Meanwhile, in the case of the specimen heated at a temperature of 400°C, the resonant frequency shift increases as the disc approaches the heating point, similar to the trend observed at 200°C, but it more abruptly shifted at the point after D4. This pattern is similarly observed in Figs. 4(d), and (e), in contrast with the critical depth of the sharply increasing frequency shift.

Fig. 5 summarizes the nonlinearity parameters calculated by Eq. (2), based on the resonant frequency shifts, as in Fig. 4. In each graph, the measurement results of four specimens cored after the heating are presented. In order to minimize the external effects, the measurement was averaged over three times for each disc. Overall, according to the tendency of the nonlinearity parameter at different depth, the nonlinearity of the concrete tends to increase as the measurement point approaches the damage source, which is presumed to be due to contact type defects. When the peak temperature is 200°C, the nonlinearity parameter also tends to increase with a constant gap, and the value increases by about 3 to 4 times as the depth is varied from D1 to D5 (Fig. 5(a)). Notably, in the case of peak temperature more than 400°C, the non-linear properties increase drastically at certain depths. In Fig. 5(b), the absolute value of the nonlinearity parameter is increased by 3 to 4 times along the depth of D1, D2, and D3, as in the case of 200°C, but the value changes by 60 to 100 times in D4 and 200 times in D5. This phenomenon is similar to the case of 600°C and 800°C (Figs. 5(c), (d)). It is presumed that, if the side of the concrete specimen is properly insulated, a microphysical and microchemical damage progression occurs at a specific depth of concrete; this means the contact type defect initiated from the concrete surface progresses to the inside of the concrete and affects the aggregates and the cement matrix (McCall and Guyer 1994). Finally, Fig. 5(e) shows the average value of the nonlinearity parameter of each specimen with different temperatures. The nonlinearity parameter of all the specimens increases with increasing peak temperature but with a larger gap of specimen 3, which is ascribed to the effect of the position of the heating source.

3.2 Relationship between compressive strength and nonlinearity parameter

The splitting tensile strength of concrete specimens was measured to evaluate the change of compressive strength, after the nonlinear resonance vibration measurements. The test was conducted according to ASTM C 496 and a universal testing machine with a capacity of 250 tonf was used (ASTM C 496 2004). Concrete discs were fixed using

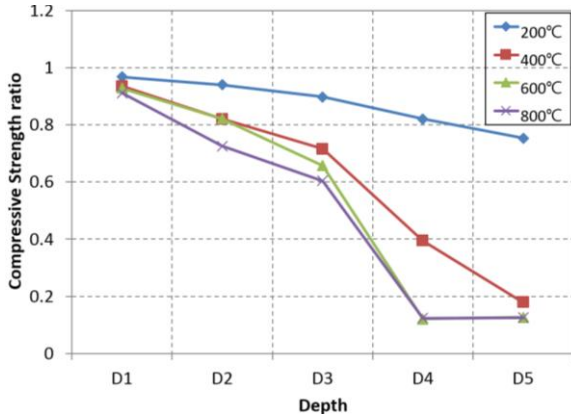


Fig. 6 Ratio of compressive strength relative to the undamaged specimen

a wood strip between the bearing blocks along the diameter, perpendicular to the ground. All processes were controlled and data were saved by a computer. The splitting tensile strength is calculated as follows

$$T_s = \frac{2F}{\pi ld} \quad (3)$$

where F is the maximum load at the point of failure, and l and d are the length and diameter of the disc, respectively. In order to calculate the compressive strength from the splitting tensile strength, the relationship between the tensile strength and the compressive strength was introduced according to the ACI 318-08 (ACI 318-08 2008).

$$f_t = 0.56f_c^{0.5} \quad (4)$$

where f_t is the splitting tensile strength and f_c is the compressive strength. Table 2 and Fig. 6 summarize the residual compressive strength ratio of the fire-damaged concrete measured and calculated according to the depth at each temperature. The splitting tensile strength was measured with four discs and is averaged for experimental accuracy. The tendency of the residual compressive strength is similar to that of the nonlinearity parameter. In the case of 200°C, D1 shows a reduction rate of about 3.3%, and D5 shows a reduction rate of about 24.8%. Also, it can be seen that the decrease gap of the compressive strength is constant with increasing depth. Meanwhile, in the case of the specimens exposed to temperature above 400°C, the residual ratio of compressive strength drastically decreases at certain depths (D4, D5) less than 50 mm, and it can be estimated that the specimens cannot fulfill their structural roles. In addition, the residual compressive strength of the specimens exposed to high temperature and damaged at depths under the critical depth shows a residual compressive strength ratio of about 0.12 to 0.2, relative to the reference specimen. Unlike the nonlinearity parameter, the reduction of the residual compressive strength is apparent even when the depth from the heating point such as D1 and D2 is large, and the relative difference of the values is also larger. However, there is a similar tendency to the rapid change at critical depth and it can be considered

Table 2 Summary of residual compressive strength estimation

Peak Temperature (°C)	Depth (mm)	Sample 1 (MPa)	Sample 2 (MPa)	Sample 3 (MPa)	Sample 4 (MPa)	Average (MPa)	Relative value
Ref	-	29.5	-	-	-	29.5	1
200	D1, 125	28	27	25	27	26.75	0.91
	D2, 100	27	26	27	25	26.25	0.89
	D3, 75	24	22	21	20	21.75	0.74
	D4, 50	22	19	23	18	20.5	0.69
	D5, 25	19	20	16	18	18.25	0.62
400	D1	20	18	19	16	18.25	0.62
	D2	16	15	18	15	16	0.54
	D3	14	14	16	15	14.75	0.5
	D4	5	4.8	6.2	3.9	4.975	0.17
	D5	2.1	3.1	2.7	1.8	2.425	0.08
600	D1	14	13	11	13	12.75	0.43
	D2	11	9	10	8	9.5	0.32
	D3	7	6	7	9	7.25	0.25
	D4	3	2	2	1	2	0.07
	D5	1	0.5	0.3	0.1	0.475	0.02
800	D1	12	13	11.7	12.2	12.225	0.41
	D2	9.8	10.1	9.3	9.6	9.7	0.33
	D3	5.2	4.4	4.9	4.6	4.775	0.16
	D4	1.2	0.9	0.7	0.9	0.925	0.03
	D5	0.2	0.1	0.08	0.1	0.12	0.01

that concrete cannot fulfill a structural function for external load and internal stress.

3.3 Dynamic elastic modulus estimated from resonant frequency values

In addition, the dynamic elastic modulus of discs was calculated with measured resonant frequencies, according to ASTM E 1876 (ASTM E 1876-09 2009). Resonance frequency measurements were performed twice for each disc, and the Poisson's ratio was calculated from the proposed standard table with the ratio of two frequencies. The dynamic elastic modulus is the average value of two natural modulus values calculated as follows

$$E_1 = [37.6991f_1^2 D^2 m(1 - \mu^2)] / (K_1^2 t^3) \quad (5)$$

$$E_2 = [37.6991f_2^2 D^2 m(1 - \mu^2)] / (K_2^2 t^3) \quad (6)$$

$$E = (E_1 + E_2) / 2 \quad (7)$$

where E is the dynamic elastic modulus, E_1 the first calculated natural modulus, E_2 the second natural modulus, f_1 is the first natural resonant frequency of the disc, and f_2 is the second natural resonant frequency of the disc. In addition, D denotes the diameter of disc, m the mass of disc, and μ the Poisson's ratio obtained as above. K is the shape

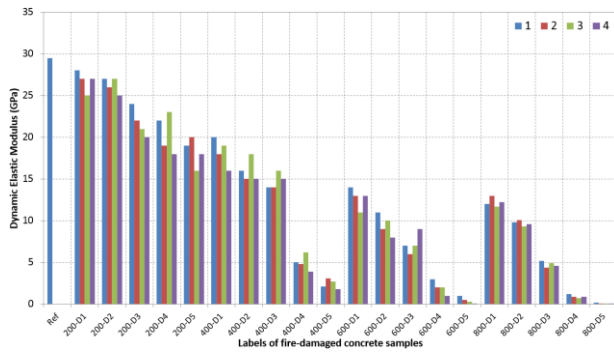


Fig. 7 Result of dynamic elastic modulus estimation

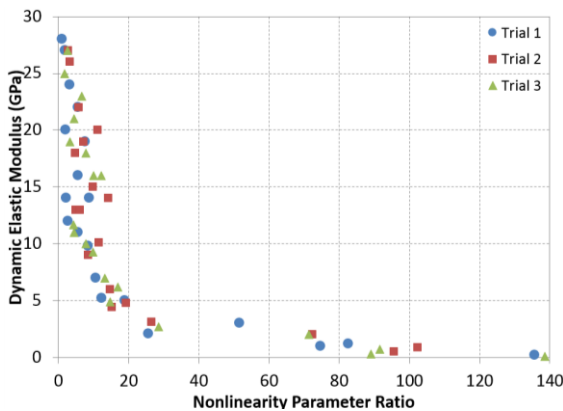


Fig. 8 Comparison between ratio of nonlinearity parameter and dynamic elastic modulus

coefficient and t is the thickness of the disc.

The values of the dynamic modulus estimated from the above equations are summarized in Fig. 7. For each condition, measurements were conducted for four discs except for the reference specimen. In the case of the reference, the modulus is measured to be about 29.5 GPa and in the case of the damaged specimen, the modulus gradually decreases according to the peak temperature and depth. First, when the peak temperature is 200°C, the average dynamic elastic modulus is about 26.8 GPa in D1, which is about 10% less than the reference specimen. Subsequently, a loss of material properties of 11% for D2, 26% for D3, 31% for D4, and 38% for D5 is observed, and the loss difference is relatively constant except for D1~D2. On the other hand, in the case of 400°C, the value at D1 is about 18.25 GPa, and the initial residual ratio shows a large reduction rate compared to the compressive strength of about 93%. This tendency is observed both in the cases of 600°C and 800°C, and it is presumed that many factors are influenced by the physiochemical change, compared to the calculation of compressive strength. The residual dynamic modulus of D3 tends to decrease to half of the initial level at D3, and decreases sharply at the depth of D4. At this point, it can be concluded that the concrete lost its structural function, with only 17% of the initial dynamic elastic modulus retained. Specimens damaged at higher temperatures also shows less than half of the modulus compared with the reference, and the residual properties gradually decrease approaching the damage source. However, at depths of 50 mm or less, the reduction rate

becomes steeper and finally the residual modulus reaches less than 1% of the initial value, which is presumed to be due to the propagation of contact-type defects.

The nonlinearity parameter and the dynamic elastic modulus were finally compared with the experimental results, as described in Fig. 8. The horizontal axis represents the relative value based on the nonlinearity parameter measured in the reference specimen, and the vertical axis represents the value of the estimated dynamic elastic modulus. In a single trial, there are 20 data from 200D1 to 800D5, and three trials are shown, except for some cases where measurements were not made due to specimen problems. As a whole, there is no deviation between the trials, and it can be seen that the residual property sharply decreases while the relative value approaches 20. This again confirms the advantages of the nonlinear technique, which sensitively reflects the initial damage of the material. In this section, however, the residual property changes suddenly even when the parameter is small, and hence it appears to be necessary to obtain the average value through additional experiments. Also, when the nonlinearity parameter ratio exceeds 20, the residual dynamic elastic modulus is about 10% of the initial level, and it can be estimated that the durability of the material is seriously degraded.

4. Conclusions

In order to estimate the material properties of fire damaged concrete, nonlinearity parameters were measured by using a nonlinear resonance vibration technique and compared according to peak temperatures and depth. Also, compressive strength and dynamic elastic modulus were measured by the ASTM method, and a comparison between the nonlinearity parameters and the material properties was performed. The experimental results and analysis can be summarized as presented below:

- The nonlinearity parameter sensitively reflects the increase of nonlinear characteristics affected by fire damage. Compared with the reference specimen, the parameter value increases slightly in the case of the relatively low temperature of 200°C, and it gradually increases with increasing peak temperature. The effect of depth is clearer, where the parameter value increases sharply at depths below D4 (under 50 mm) in all damaged specimens except the case of 200°C.
- Estimation of the residual compressive strength of fire-damaged concrete by measuring the splitting tensile strength shows a similar tendency to that of the nonlinearity parameter. As the peak temperature increases, the residual compressive strength decreases gradually, especially at depths less than 50 mm, to a 10% level relative to the initial value. This phenomenon is presumed to be caused by propagation of contact type defects into the cement matrix and aggregate region.
- The results of the dynamic elastic modulus show that the values measured at D1 for each temperature are relatively low compared with the nonlinearity parameter and compressive strength. This is ascribed to the effect of many factors during the calculation process, which is

induced from the fire damage and measurement error. However, as the peak temperature increases, the value of the dynamic elastic modulus gradually decreases, and the residual property similarly decreases rapidly below the critical depth (50 mm). According to Fig. 8, the value of the dynamic elastic modulus changes sensitively with a nonlinearity parameter less than 20. This suggests that the general tendency should be carefully determined through additional experiments. Additionally, in the case of specimens with parameter values more than 20, the residual property ratio is less than 10%, and it is estimated that structural function cannot be fulfilled.

With the experimental results of this study, the possibility of using a nonlinear resonance vibration technique for evaluating the depth-dependent material properties of fire-damaged concrete was verified. With additional experiments and improvement of accuracy, the applicability of this technique can be increased for in-situ cases.

Acknowledgments

This research was supported by a grant(17RDRP-B076268-04) from R&D Program funded by Ministry of Land, Infrastructure and Transport of Korean government and this work is supported by the Korea Agency for Infrastructure Technology Advancement(KAIA) grant funded by the Ministry of Land, Infrastructure and Transport (Grant 13IFIP-C113546-01).

References

- ACI(American Concrete Institute) (1989), *ACI 216R-89: Guide for Determining the Fire Endurance of Concrete Elements*, Farmington Hills, Michigan, U.S.A.
- ACI (1997), *ACI Committee 216: Standard Method for Determining Fire Resistance of Concrete and Masonry Construction Assemblies*, Farmington Hills, Michigan, U.S.A.
- ACI (1998), *ACI Committee 228: Nondestructive Test Methods for Evaluation of Concrete in Structures*, Farmington Hills, Michigan, U.S.A.
- ACI (2008), *ACI Committee 318: Building Code Requirements for Structural Concrete and Commentary*, Farmington Hills, Michigan, U.S.A.
- Alonso, C. and Fernandez, L. (2004), "Dehydration and rehydration processes of cement paste exposed to high temperature environments", *J. Mater. Sci.*, **39**(9), 3015-3024.
- ASTM C 39-01 (2001), *Standard Test Method for Compressive Strength of Cylindrical Concrete Specimens*, Annual Book of ASTM Standards, ASTM International, West Conshohocken, Pennsylvania, U.S.A.
- ASTM C 496 (2004), *Standard Test Method for Splitting Tensile Strength of Cylindrical Concrete Specimens*, Annual Book of ASTM Standards, ASTM International, West Conshohocken, Pennsylvania, U.S.A.
- ASTM E 1876 (2009), *Standard Test Method for Dynamic Young's Modulus, Shear Modulus, and Poisson's Ratio by Impulse Excitation of Vibration*, ASTM International, West Conshohocken, Pennsylvania, U.S.A.
- Bazant, J.P. and Kaplan, M.F. (1996), *Concrete at Higher*

- Temperatures: Material Properties and Mathematical Models*, Longman, London, U.K.
- Choi, E.G., Kim, H.S. and Shin, Y.S. (2012), "Performance of fire damaged steel reinforced high strength concrete (SRHSC) columns", *Steel Compos. Struct.*, **13**(6), 521-537.
- Cloni, P., Croce, P. and Salvatore, W. (2001), "Assessing fire damage to RC elements", *Fire Saf. J.*, **42**(6), 461-472.
- Gomez, C.Q., Garcia, F.P., Arcos, A., Cheng, L., Kogia, M. and Papeliias, M. (2017), "Calculus of the defect severity with EMATs by analyzing the attenuation curves of the guided waves", *Smart Struct. Syst.*, **19**(2), 195-202.
- Guyer, R.A. and Johnson, P.A. (1999), "Nonlinear mesoscopic elasticity: Evidence for a new class of materials", *Phys. Tod.*, **52**(4), 30-36.
- Handoo, S., Agarwal, S. and Agarwal, S. (2002), "Physicochemical, mineralogical, and morphological characteristics of concrete exposed to elevated temperatures", *Cement Concrete Res.*, **32**(7), 1009-1018.
- Jhang, K.Y. (2009), "Nonlinear ultrasonic techniques for nondestructive assessment of micro damage in material: A review", *J. Prec. Eng. Manuf.*, **10**(1), 123-135.
- Kim, J.H. and Kwak, H.G. (2008), "Nondestructive evaluation of elastic properties of concrete using simulation of surface waves", *Comput. Aid. Civil Inf.*, **23**(8), 611-624.
- McCall, K. and Guyer, R. (1994), "Equation of state and wave propagation in hysteretic nonlinear elastic materials", *J. Geophys. Res.*, **65**(11), 651-659.
- Park, S.J., Kim, G.J. and Kwak, H.G. (2017), "Characterization of stress-dependent ultrasonic nonlinearity variation in concrete under cyclic loading using nonlinear resonant ultrasonic method", *Constr. Build. Mater.*, **145**, 272-282.
- Park, S.J., Park, G.K., Yim, H.J. and Kwak, H.G. (2015), "Evaluation of residual tensile strength of fire-damaged concrete using a non-linear resonance vibration method", *Mag. Concrete Res.*, **67**(5), 235-246.
- Payan, C., Garnier, V., Moysan, J. and Johnson, P. (2007), "Applying nonlinear resonant ultrasound spectroscopy to improving thermal damage assessment in concrete", *J. Acoust. Soc. Am.*, **121**(4), EL125-EL130.
- Tang, C.W. (2017), "Fire resistance of high strength fiber reinforced concrete filled box columns", *Steel Compos. Struct.*, **23**(5), 611-621.
- Van Den Abeele, K.E.A., Carmeliet, J., Ten Cate, J.A. and Johnson, P.A. (2000b), "Nonlinear elastic wave spectroscopy (NEWS) techniques to discern material damage, part II: Single-mode nonlinear resonance acoustic spectroscopy", *Res. Nondestr. Eval.*, **12**(1), 31-42.
- Van Den Abeele, K.E.A., Johnson, P.A. and Sutin, A. (2000a), "Nonlinear elastic wave spectroscopy (NEWS) techniques to discern material damage, part I: Nonlinear wave modulation spectroscopy (NWMS)", *Res. Nondestr. Eval.*, **12**(1), 17-30.
- Van Den Abeele, K.E.A., Sutin, A., Carmeliet, J. and Johnson, P.A. (2001), "Micro-damage diagnostics using nonlinear elastic wave spectroscopy (NEWS)", *NDT&E Int.*, **34**(4), 239-248.
- Yang, H., Lin, Y., Hsiao, C. and Liu, J.Y. (2009), "Evaluating residual compressive strength of concrete at elevated temperatures using ultrasonic pulse velocity", *Fire Saf. J.*, **44**(1), 121-130.
- Yu, K. and Lu, Z. (2015), "Influence of softening curves on the residual fracture toughness of post-fire normal-strength concrete", *Comput. Concrete*, **15**(2), 199-213.
- Zhang, G., Kodur, V., Hou, W. and He, S. (2017), "Evaluating fire resistance of prestressed concrete bridge girders", *Struct. Eng. Mech.*, **62**(6), 663-674.